

Lignocellulosic Fiber-Reinforced Keratin Polymer Composites

Justin R. Barone

Published online: 28 August 2009
© Springer Science+Business Media, LLC 2009

Abstract Short fiber reinforced polymer composites were prepared from lignocellulose fibers and feather keratin polymer (FKP). The FKP matrix was prepared from the reactive processing of poultry feather keratin, glycerol, water, and sodium sulfite. Lignocellulose fibers of varying source, length, and mass fraction were used and it was found that positive reinforcement of FKP was affected by all three. Positive reinforcement was defined as an increase in elastic modulus when normalized by FKP with the same amount of glycerol but no fibers. Positive reinforcement was only able to occur for modulus but not stress at break indicating that the composites were of high physical properties only under small deformations. At large deformations, fiber pull-out was observed in the composites using scanning electron microscopy. The most likely origin of this behavior appeared to be from weak fiber–polymer interactions dominated by friction and rationalized by a force balance across the fiber–polymer interface. High fiber loadings were shown to be reinforcing because of the formation of a network of lignocellulose fibers. The addition of lignocellulose fibers increased the thermal stability of the material.

Keywords Bio-based polymers · Composites · Properties · Keratin · Lignocellulose

Introduction

Currently, there is a large effort to develop polymers from renewable sources in direct response to the price of

petroleum. Polymers and fuels are two products of petroleum refining. Petroleum is not renewable on reasonable time scales. In 2008, the price of petroleum-based polymers rose faster than gasoline as more petroleum supply was diverted into fuel and less into polymers. This made polymers more valuable than fuel, i.e., a kg of polyethylene cost about \$1.98 while a kg of gasoline cost about \$1.08 (<http://www.plasticsnews.com/subscriber/resin/price1.html>); Using a density of 737.22 kg/m³, gasoline at \$3.00/gal is \$1.08/kg). This showed that polymers were being compromised in favor of fuel. Polylactic acid (PLA) is currently the largest volume renewable polymer sold commercially and is made from the fermentation of cornstarch. PLA has the potential to be cost and property competitive with some petroleum-based polymers. Agriculture is diverting more corn supply into ethanol (fuel) and less into food and PLA and demand for fuel increased corn prices to an all time high just like petroleum [1]. Concurrently, PLA prices increased [2]. Food prices also increased because most animals eat corn and many food products are made from cornstarch and corn oil. In agriculture, polymers *and* food were compromised in favor of fuel, whereas only polymers were compromised in the petroleum-based industry. Proteins and polysaccharides that are the by-product of agriculture and food processing are not derived from petroleum and are not a primary food product so they do not compete with food or fuel and will not be compromised when demand for those products rises. Proteins contain nitrogen and sulfur and cannot be directly converted to fuel very easily. So making polymers from by-products could be very cost effective if suitable processing methods can be found.

After poultry processing, there is about 1.5 billion kilograms of dry poultry feathers that require disposal in the U.S. annually [3]. We have shown that these feathers

J. R. Barone (✉)
Biological Systems Engineering Department, Virginia Tech,
303 Seitz Hall (0303), Blacksburg, VA 24061, USA
e-mail: jbarone@vt.edu

can be easily converted into useful polymers using standard polymer processing methods [4, 5]. In addition, many lignocellulosic materials are available in the form of, for example, wheat straw, corn stover, hemp, flax, etc. It is not as easy to convert these lignocellulosics to polymers in an environmentally friendly way. Therefore, it may be better to use lignocellulosics as-is and their fibrous structure makes them advantageous for use in composites. Many polymers are sold with additives such as fillers that add strength, stiffness, and dimensional stability to the polymers. Lignocellulosic fibers have elastic modulus and stress at break values that are higher than FKP [6, 7]. So it may be advantageous to use lignocellulosic fibers in FKP matrices to make 100% bio-based composites.

There is a large body of literature on the use of lignocellulosic fiber/polymer composites where the polymers are typically polyolefins or bio-based polyesters [8 and references therein, 9]. Polyolefins are petroleum-derived so these composites are not 100% bio-based. Bio-based polyesters are expensive and have limited application because most have glass transition temperatures above room temperature. Easy to produce and inexpensive polymers can be made through the plasticization of biopolymers with small molecular weight polar molecules such as glycerol [4 and references therein, 10 and references therein, 11, 12]. Glycerol-plasticized biopolymers represent a very well studied and commercially useful class of polymers. These plasticized materials are usually very flexible and tough but the modulus and stress at break of the biopolymer is severely compromised. All plasticized polymers suffer from diffusion problems. For example, plasticized polyvinyl chloride will eventually embrittle from loss of plasticizer. The diffusion is obviously hastened by higher temperatures. In addition, glycerol is hydrophilic and will diffuse out of the polymer in humid environments and be replaced by the less efficient plasticizer water.

To overcome deficiencies in modulus and strength, the biopolymer can be cross-linked with chemicals or enzymes [13–16]. This typically results in a slight increase in physical properties but the chemicals used for cross-linking may detract from the overall environmental-friendliness of the material. Another method is to reinforce the plasticized biopolymer with fibers of higher modulus, especially biological fibers to keep the material 100% bio-based. This has been done recently using lignocellulose or pure cellulose reinforcement and plasticized starch or protein [10, 16–21]. In general, adding cellulosic reinforcement, whether nano-scale or macro-scale, resulted in increased modulus and stress at break. Unplasticized polysaccharides and proteins have also been used as composite matrices for lignocellulose- and cellulose-reinforced composites and nanocomposites [22–24]. Results in these instances appear

to be mixed with microcrystalline cellulose increasing modulus, stress at break and strain at break for silk matrices and sisal fibers increasing the physical properties of benzylated sawdust matrices, but corn fiber adversely affected the physical properties of starch/PVA matrices.

In this article, lignocellulose-based fibers obtained from different plant materials, (namely, wheat straw, corn stalk, coffee chaff, flax, kenaf, banana, and hemp), were separately incorporated into feather keratin polymer at weight percentages of 0–40 wt%. Following mixing, tensile bars were prepared and tested in uniaxial tension to assess elastic modulus (E), stress at break (σ_b), and strain at break (ϵ_b). Scanning electron micrographs (SEM) of the fracture surfaces denoted fiber–polymer interactions and fiber orientation. Fourier transform infrared spectroscopy (FT-IR) and thermogravimetric analysis (TGA) denoted fiber–polymer interactions and composite thermal stability.

Materials and Methods

Feather Keratin Polymer (FKP)

Cleaned, chopped feather keratin was obtained from Featherfiber[®] Corporation (Nixa, MO). The feather keratin was ground on a Retsch PM400 planetary ball mill. Each of four 500 mL stainless steel grinding vessels was loaded with 15 g of feather keratin so that the material occupied about a quarter of the vessel's volume. The grinding media were four 4 cm diameter stainless steel spheres for a total of 1,132 g grinding media. Grinding proceeded at 200 rpm for 30 min. The average particle size of the ground feather keratin was 53 μm [4, 5]. Sodium sulfite (Na_2SO_3 , Mallinckrodt, reagent grade, mol. wt. = 126.04 g/mol, density = 2.63 g/cm³) was dissolved in de-ionized water (DI-H₂O) at a concentration of 3 wt% of total feather keratin content to give a solution with pH = 9.9. This concentration was found to give the lowest apparent viscosity during processing most likely because of full reduction of cystine bonds between keratin molecules [5]. Dissolution of sodium sulfite was aided by stirring. Glycerol [$\text{C}_3\text{H}_5(\text{OH})_3$, Sigma–Aldrich, 99+%, mol. wt. = 92.1 g/mol, boiling point = 290 °C, density = 1.26 g/cm³] was added to the aqueous solution and further mixed for 10 min. The ground feather keratin was added to a Brabender mixing head at 40 °C with blades rotating at 50 rpm. The liquid was added and mixed for 15 min to obtain a blend of 50:30:18.5:1.5 wt% of feather keratin:glycerol:DI-H₂O: Na_2SO_3 .

Lignocellulose Fibers

Corn stalk, wheat straw, and banana fiber were obtained from Tyson Foods, Inc. Coffee chaff was received from

Millstone Coffee. Coffee chaff was the husk of the coffee bean removed during roasting and is a major waste product of the coffee industry. Hemp, flax, and kenaf were received in long fiber form from the USDA-ARS. Each as-received material was ground and sieved to 53 μm particles as described above. In addition, the wheat straw fraction that remained above the 246 and 589 μm sieves was retained to further study the effect of fiber length on composite properties.

Composite Preparation

Composites were prepared similarly to the FKP outlined above. The first study involved mixing 30 wt% 53 μm long fibers into 70 wt% FKP to observe the reinforcing effect of each type of fiber on the composite. The second study involved mixing 53 μm long wheat straw fibers from 0 to 40 wt% to observe the effect of fiber loading on composite properties. The final experiment involved mixing 30 wt% wheat straw fibers of 53, 246, and 589 μm length into 70 wt% FKP to observe the effect of fiber length on composite properties. The melt temperature was monitored independently and ranged from 43 $^{\circ}\text{C}$ for the pure FKP to 63 $^{\circ}\text{C}$ for 30% 589 μm wheat straw loading.

Following mixing, 5 g of each sample was placed between two Teflon-coated aluminum foil sheets and pressed in a Carver Press Autofour/30 Model 4394 at 120 $^{\circ}\text{C}$ and 7.8 MPa for 2 min. The composite was then removed and air-cooled to room temperature. The conditions for composite preparation were based on previous studies that minimized fiber attrition and shear heating, which were factors that could degrade the composite, and maximized feather keratin polymer formation, which if incomplete could affect composite properties [4, 5, 25, 26].

Composite Testing

Uniaxial tensile testing was performed using a Com-Ten Industries 95 RC Test System at a test speed of 2.54 cm/min. Samples were 10 cm long by 2.5 cm wide by 0.025–0.030 cm thick and a gage length of 5 cm was used. A minimum of ten samples of each composite was tested. Elastic modulus, E , was defined as the slope of the initial linear portion of the stress–strain curve after correcting for the toe region. The stress at break, σ_b , and strain at break, ε_b , were defined as the maximum stress and strain the sample withstood before breaking.

Scanning Electron Microscopy (SEM)

The fracture surfaces were excised from the failed tensile bars using a scalpel blade and transferred into a modified specimen carrier. The specimen carrier was known as an

“indium vise” because the dissected pieces were clamped between sheets of indium metal and plunge cooled in liquid nitrogen to -196 $^{\circ}\text{C}$. The cooled holder was then transferred to an Oxford CT1500 HF cryo-preparation system attached to a Hitachi S-4100 scanning electron microscope (SEM). The sample temperature was raised to -90 $^{\circ}\text{C}$ for 10 min to remove surface water from the sample surface. The sample was then cooled to below -120 $^{\circ}\text{C}$ and coated with approximately 5 nm of platinum metal using a magnetron sputter coater. Coated samples were transferred to the cold stage in the SEM at -170 $^{\circ}\text{C}$ and observed with an electron beam accelerating voltage of 2 KV.

Fourier Transform Infrared (FT-IR) Spectroscopy

Cellulose fiber and composite samples were analyzed using a Thermo Electron 6700 FT-IR in ATR mode. Sixty-four scans at a resolution of 4 cm^{-1} were used. Background spectra were obtained before each scan and blanks run between each sample scan to allow for quantitative FT-IR analysis.

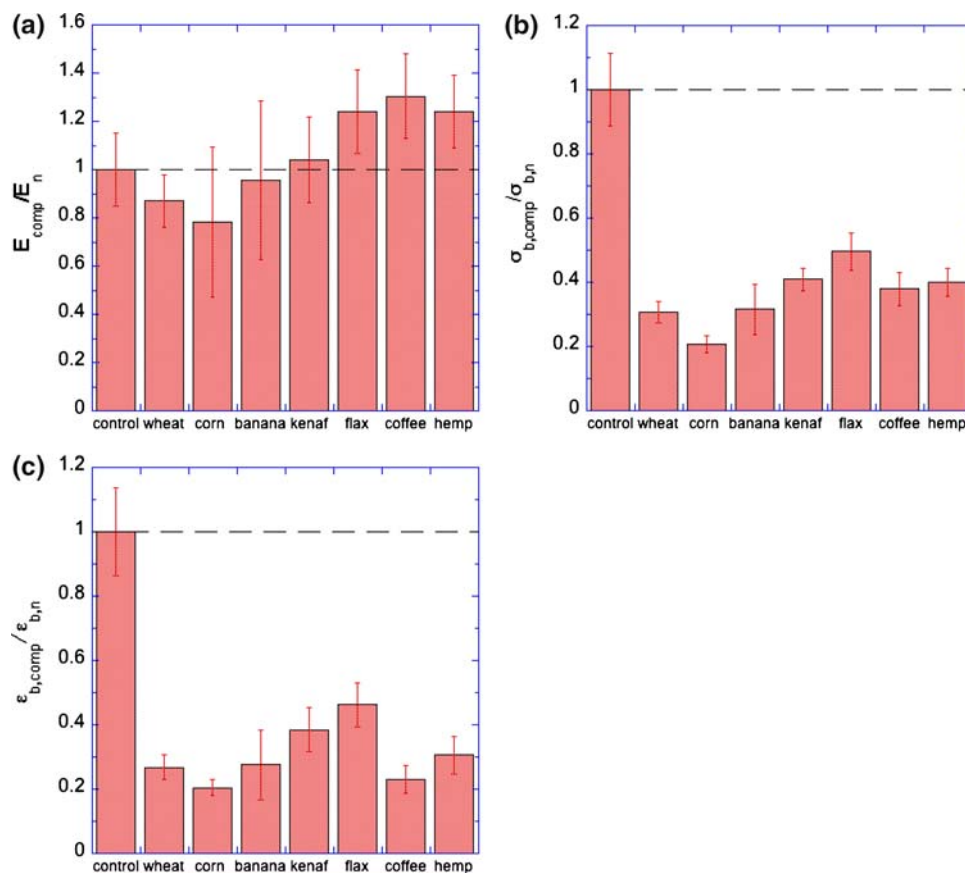
Thermal Analysis

Thermogravimetric analysis (TGA) was performed on a TA Instruments SDT Q600 DSC/TGA using sample sizes of 10 mg and a heating rate of 10 $^{\circ}\text{C}/\text{min}$.

Results and Discussion

Figure 1a–c shows the effect of different 53 μm long cellulose fiber types on FKP matrix composite properties at 30 wt% fiber loading. The composite properties (E_{comp} , $\sigma_{b,\text{comp}}$, and $\varepsilon_{b,\text{comp}}$) were normalized by the corresponding properties of FKP with the *same amount of glycerol but no fiber* (E_n , $\sigma_{b,n}$, and $\varepsilon_{b,n}$, which were obtained from [4]). Therefore, this analysis showed the effect of adding lignocellulose fibers to FKP while keeping the amount of plasticizer constant and demonstrated if fibers acted as a positive reinforcement outside of just lowering the relative amount of glycerol in the sample as a whole. When filler was added to plasticized polymers, the amount of plasticizer relative to solids decreased unless the glycerol:solids ratio was adjusted to remain constant. Simply lowering the glycerol content will increase modulus and stress at break [4]. In the absence of normalization, E_{comp} and $\sigma_{b,\text{comp}}$ increased over the respective values for FKP of composition 50:30:18.5:1.5 feather keratin:glycerol:DI- H_2O : Na_2SO_3 (FKP matrix of 0 wt% fibers) while $\varepsilon_{b,\text{comp}}$ decreased. This was expected polymer composite behavior and was also observed in composites of plasticized starch or protein and cellulose-based fiber reinforcement [16, 17, 19–21].

Fig. 1 Normalized **a** Elastic modulus, E , **b** stress at break, σ_b , and **c** strain at break, ε_b , for 30 wt% 53 μm long fiber composites for varying cellulosic fibers in FKP



Positive reinforcement was observed for kenaf, hemp, coffee chaff, and flax as $E_{\text{comp}}/E_n > 1$ but $\sigma_{b,\text{comp}}/\sigma_{b,n} < 1$ for all fibers. Therefore, lignocellulosic fibers of similar size and loading in the same polymer matrix do not have the same reinforcing ability [6] (Table 1).

The lack of reinforcement could have several origins including too low of a fiber loading, lack of sufficient load transfer because the fiber length was too short, or low fiber/polymer interactions perhaps related to slight differences in the chemical composition of the lignocellulosic fiber. To explore the fiber loading dependence, wheat straw (WS) fiber was chosen because $E_{\text{comp}}/E_n < 1$ and $\sigma_{b,\text{comp}}/\sigma_{b,n} < 1$. Figure 2a shows the non-normalized composite properties

increased with increasing fiber content. Figure 2b shows the normalized composite results for 53 μm long wheat straw fiber loadings from 0 to 40 wt%. $E_{\text{comp}}/E_n > 1$ at high fiber loadings but $\sigma_{b,\text{comp}}/\sigma_{b,n} < 1$ for all fiber loadings. TGA weight loss experiments showed that the addition of lignocellulosic fibers increased the thermal stability of the bio-based composites. For example, at 300 $^{\circ}\text{C}$, 60% of the weight of FKP was lost while only 40% of the 40 wt% wheat straw composite weight was lost as shown in Fig. 3a. Thermal stability was perhaps better examined using TGA first derivative with temperature, $d(\%W)/dT$. Water and glycerol evaporated at ca. 75 and 200 $^{\circ}\text{C}$, respectively, and peaks appeared accordingly. Higher fiber loading meant less glycerol therefore the 200 $^{\circ}\text{C}$ was smaller. The stability of the composites can be quantified by the peaks between 300 and 325 $^{\circ}\text{C}$, which shifted to higher temperatures at higher fiber loadings. Biopolymers are typically temperature sensitive and one simple way to increase thermal stability may be the addition of lignocellulose fibers.

The results of Fig. 2 indicated that fiber length might be an issue. Wheat straw fibers of 53, 246, and 589 μm lengths (aspect ratios, $L/D = 6, 25,$ and $62,$ respectively, with D determined from SEM micrographs of the fibers) at 30 wt% fiber loading were analyzed and the normalized results are shown in Fig. 4. While there was only reinforcement seen in E , a critical aspect ratio where

Table 1 Absolute properties of fiber-reinforced composites in Fig. 1

Sample	E (GPa)	SD	σ_b (MPa)	SD	ε_b (cm/cm)	SD
Control	0.046	0.007	8.600	0.970	0.370	0.051
Wheat	0.040	0.005	2.634	0.285	0.099	0.014
Corn	0.036	0.014	1.776	0.228	0.076	0.010
Banana	0.044	0.015	2.713	0.663	0.102	0.040
Kenaf	0.048	0.008	3.513	0.308	0.142	0.025
Flax	0.057	0.008	4.261	0.506	0.171	0.025
Coffee	0.060	0.008	3.259	0.453	0.085	0.016
Hemp	0.057	0.007	3.473	0.366	0.113	0.022

Fig. 2 **a** Non-normalized and **b** normalized composite properties for wheat straw fiber in FKP as a function of fiber loading

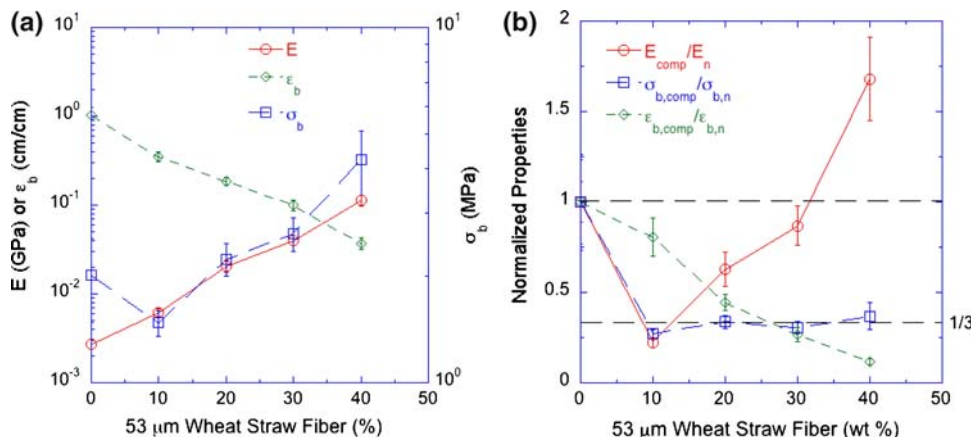


Fig. 3 TGA **a** weight loss and **b** first derivative with temperature, $d(\%W)/dT$, results for 53 μm long wheat straw fiber composites as a function of fiber loading

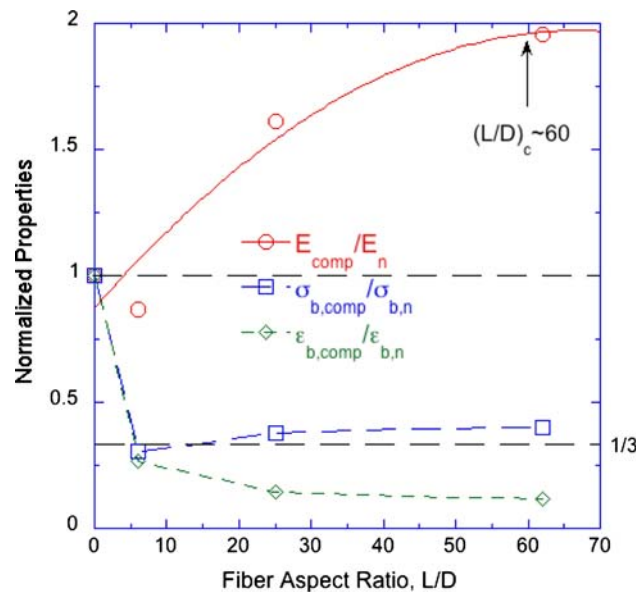
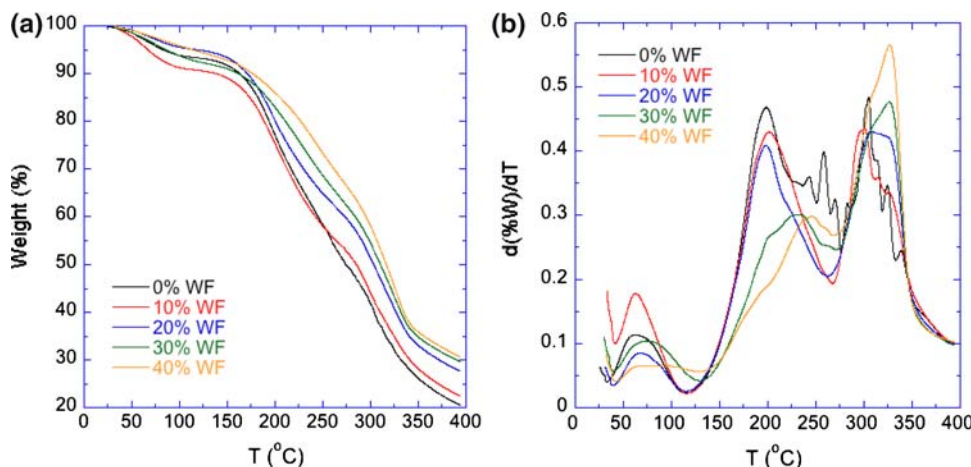


Fig. 4 Normalized properties of 30 wt% wheat straw composites in FKP as a function of fiber aspect ratio (L/D)

reinforcement did not increase further with increasing fiber aspect ratio could be realized at about $(L_c/D)_f \sim 60$. This indicated that the fibers needed to be about 580 μm long

for sufficient reinforcement of the FKP matrix. As a comparison, composite data in ref. [21] were normalized by the protein:glycerol data without fibers and showed that reinforcement occurred for all fiber contents of 15 mm long fibers, 20 and 30 wt% fibers of 10 mm length, and no reinforcement for the 5 mm long fibers. So the observed behavior may be generic for composites of lignocellulose fibers in plasticized protein matrices.

An interesting observation was that the normalized stress at break in Figs. 2b and 4 both showed the same behavior, i.e., $\sigma_{b,\text{comp}}/\sigma_{b,n} \sim 1/3$. At $\epsilon^* = \text{constant} < 0.02$, the stress state in the composite is higher than the stress state in the FKP matrix without fiber because $E_{\text{comp}} > E_n$ at ϵ^* , i.e., $\sigma = E\epsilon^*$ and therefore $\sigma_{\text{comp}} > \sigma_n$ as shown in Fig. 5 for typical stress–strain curves of the two materials at constant glycerol concentration. So load was borne by the fiber in the composite at low strains because there was good stress transfer across the fiber–polymer interface. Failure in the composite occurred at $\sigma_{b,\text{comp}} = \sigma_{b,n}/3$. Assuming the composite was incompressible and the fiber and polymer were strained equally, the shear stress generated in the polymer matrix parallel to the fiber was $\tau_{\text{max}} \sim \sigma_{b,n}/3 \sim 11.5/3 \sim 3.8$ MPa. Shear lag theory can be used to relate fiber properties to overall mechanical failure of the

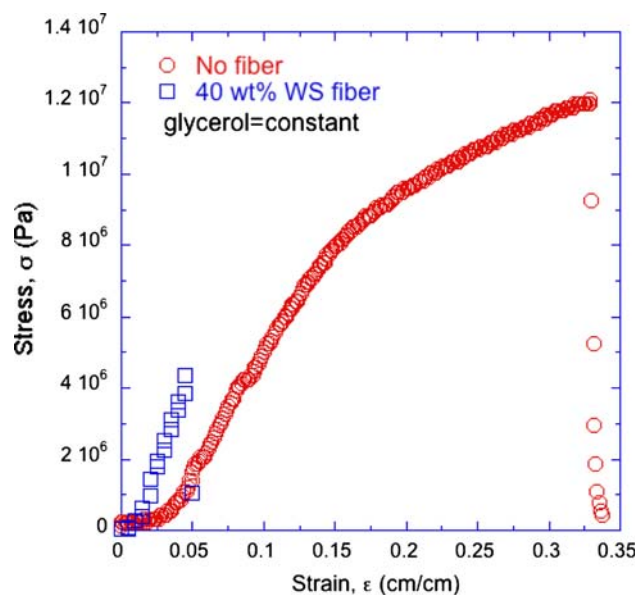


Fig. 5 Stress–strain (σ – ϵ) curves for FKP and FKP with 40 wt% 53 μm wheat straw fiber at a constant glycerol concentration

composite [27–29]. A force balance across the fiber–polymer interface yielded

$$\left(\frac{L_c}{D}\right)_f = \frac{\sigma_{b,f}}{2\tau_i} \quad (1)$$

where $\sigma_{b,f}$ was the stress at break of the fiber, τ_i was the maximum shear stress that the interface could support, and $(L_c/D)_f$ was the critical fiber length to load the fiber to its stress at break. Using $(L_c/D)_f = 6$ and $\sigma_{b,f} = 59$ MPa, $\tau_i \sim 4.9$ MPa $\sim \tau_{\text{max}}$ [30]. In other words, the shear stress generated in the matrix was transferred to the fiber up to τ_i and then fiber pull-out occurred, which ended up being the major failure mechanism of the composites. SEM micrographs revealed fibers pulled-out of the matrix and clear spaces where fibers used to reside as shown in Fig. 6a. Voids around the fiber are shown in Fig. 6b with no fracture of fibers in the plane.

For short fibers, i.e., $(L/D)_f < (L_c/D)_f$, reinforcement occurred at WS fiber mass fractions greater than $m_f^* > 0.33$ as shown in Fig. 2b. So there was a second mechanism for reinforcement besides stress transfer from matrix to long fibers. SEM micrographs revealed a clear change in the fracture surface between 30 wt% WS fiber and 40 wt% WS fiber as shown in Fig. 7a and b. The 40 wt% WS fiber fracture surface appeared flatter and more cohesive while the 30 wt% WS fiber fracture surface was rougher with more voids and pulled-out fibers. This could be similar to cellulose fiber interlocking at large fiber contents, which is important for the physical properties of paper. For this to happen, there would have to be enough fibers for them to interact with one another. To see if this was possible, the

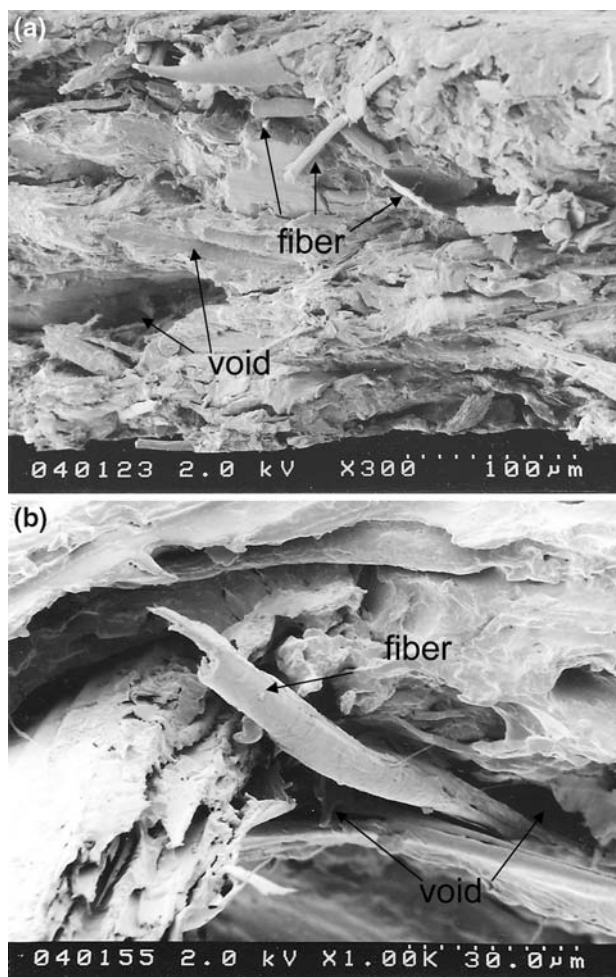


Fig. 6 Thirty weight percent wheat straw fiber in FKP at **a** $\times 300$ magnification and **b** $\times 1,000$ magnification

average distance between the fibers was estimated as a function of fiber volume fraction, ϕ_f . The volume of one fiber was $V_f = 3.9 \times 10^{-9}$ cm^3 using $L = 5.3 \times 10^{-3}$ cm, $D = 9.7 \times 10^{-4}$ cm and treating the fibers as cylinders. The total volume of fibers in the composite was $V_{f,T} = 5^*(m_f/\rho_f)$, where ρ_f was the fiber density of 1.4 g/cm^3 , m_f was the mass fraction of fiber, and each composite sample was 5 g [6]. So the total number of fibers in the composite, $N_{f,T}$, was $N_{f,T} = V_{f,T}/V_f$. The composite density, ρ_c , can be found from

$$\rho_c = \left(\frac{m_f}{\rho_f} + \frac{m_{FKP}}{\rho_{FKP}}\right)^{-1} \quad (2)$$

where ρ was density, m was mass fraction, f was fiber and FKP was feather keratin polymer matrix [27]. While the density of the feather was about 0.89 g/cm^3 , the feather was a porous structure and the density of the keratin comprising the feather was higher. The density of the keratin was estimated to be 1.47 g/cm^3 [31]. The density of the

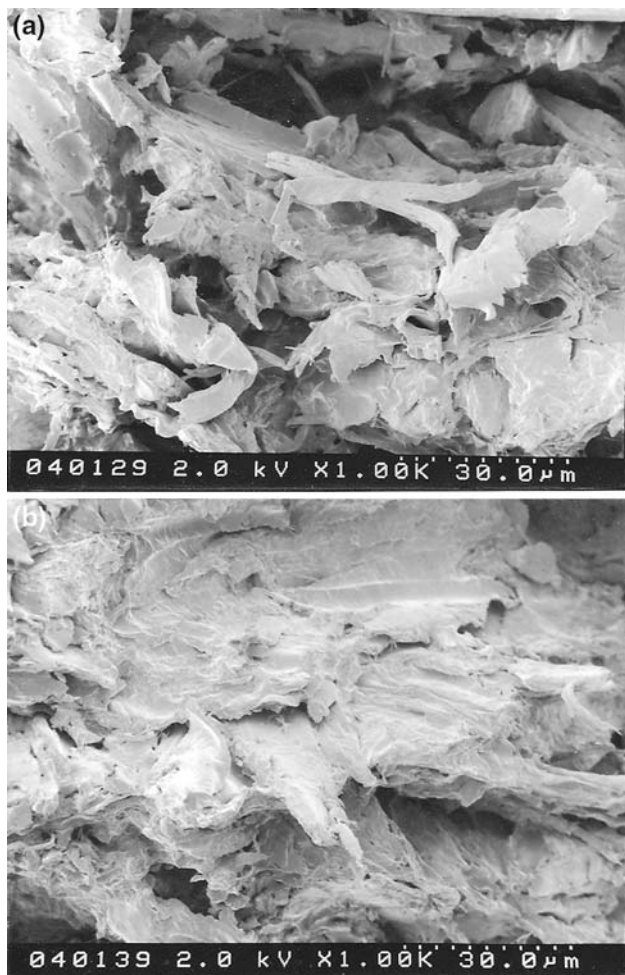


Fig. 7 Transition from **a** 30 wt% to **b** 40 wt% wheat straw fiber in FKP

FKP was estimated using an equation similar to Eq. 2 with feather keratin, glycerol, water, and sodium sulfite as the components and was $\rho_{FKP} = 1.30 \text{ g/cm}^3$. Some water was lost during compounding but some was regained afterwards from ambient conditions so the amount of water was assumed constant for simplicity. Total composite volume, V , was therefore $V = 5/\rho_c$. The average distance between fibers can be defined as $(N_{f,T}/V)^{-1/3}$. This analysis was similar to one in ref. [32] for liquid crystalline materials. The results are plotted in Fig. 8 as a function of fiber volume fraction, $\phi_f = (\rho_c - \rho_{FKP})/(\rho_f - \rho_{FKP})$, and it can be seen that severe crowding of the system occurred at $\phi_f^* \sim 0.32$ (corresponding to $m_f^* \sim 0.33$). This was the point where the fibers were packed together closely and this type of system can have reinforcement because of fiber/fiber interactions just like in paper.

FT-IR examination of the lignocellulosic fibers showed differences in the lignin/hemicellulose/cellulose ratio in each fiber as evidenced by the $\nu(\text{C}-\text{C})$ peaks at $1,510 \text{ cm}^{-1}$ and $\nu(\text{C}=\text{O})$ peak at $1,250 \text{ cm}^{-1}$ from phenol; the $\nu(\text{C}=\text{O})$

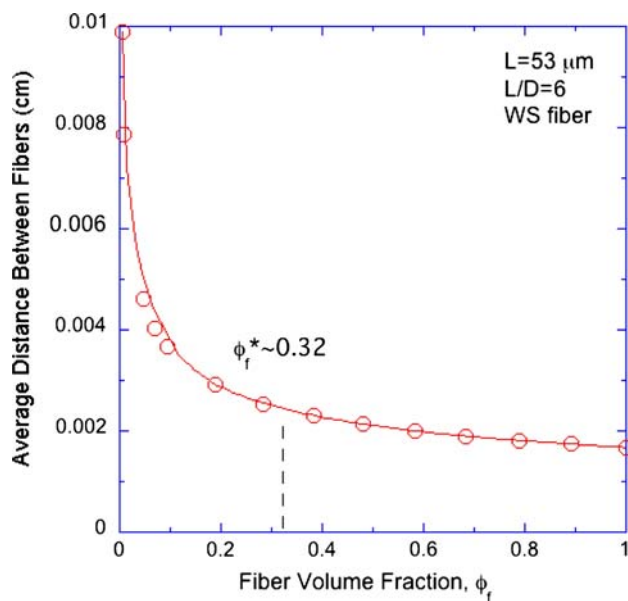


Fig. 8 Average distance between fibers vs. fiber volume fraction, ϕ_f

at $1,720 \text{ cm}^{-1}$ from hemicellulose; and the $\nu(\text{C}-\text{O})$ peak at $1,050 \text{ cm}^{-1}$ from cellulose. However, neither definitive trend was observed between the chemical nature of the lignocellulose fiber as measured by FT-IR and the reinforcing ability of the fiber nor were any significant differences found between the spectra of the composites in Fig. 1 that indicated one composite was better than another. FT-IR results did indicate that some chemical interactions between the keratin matrix and fibers might have enhanced reinforcement at high fiber loadings and long fiber lengths. The $\nu(\text{O}-\text{H}, \text{N}-\text{H})$ at $3,300 \text{ cm}^{-1}$ and symmetric and asymmetric alkene stretches from $2,960$ to $2,850 \text{ cm}^{-1}$ all decreased in intensity with increased fiber loading. Adding more fiber simply reduced these vibrations because there was less protein and more tightly bound OH and CH_2 from the fiber. Figure 9 shows the Amide region of the composites for various loadings of wheat straw fiber in FKP. New peaks appeared around $1,200$, $1,160$, and 600 cm^{-1} with increased fiber loading (the peaks were most prominent in the 30 and 40 wt% composites). These peaks also appeared more prominently as fiber length increased at 30 wt% WS fiber. So, although the data are not shown, the phenomenon described henceforth appears to be the same for moderate loadings of very long fibers. In wheat straw fiber, the $1,160 \text{ cm}^{-1}$ peak was prominent, the $1,200 \text{ cm}^{-1}$ peak was a shoulder on the $1,250 \text{ cm}^{-1}$ peak, and the 600 cm^{-1} peak did not exist. None of the peaks appeared in the lower loading composite spectra. The $1,200$ and $1,160 \text{ cm}^{-1}$ peaks were assigned to $\nu(\text{C}-\text{O})$ in lignin phenols in the fiber and the 600 cm^{-1} peak to $\delta_{\text{oop}}(\text{O}-\text{H})$ [33]. Given the appearance of phenolic ring peaks the 600 cm^{-1} peak probably originated in hydroxyls on the phenol

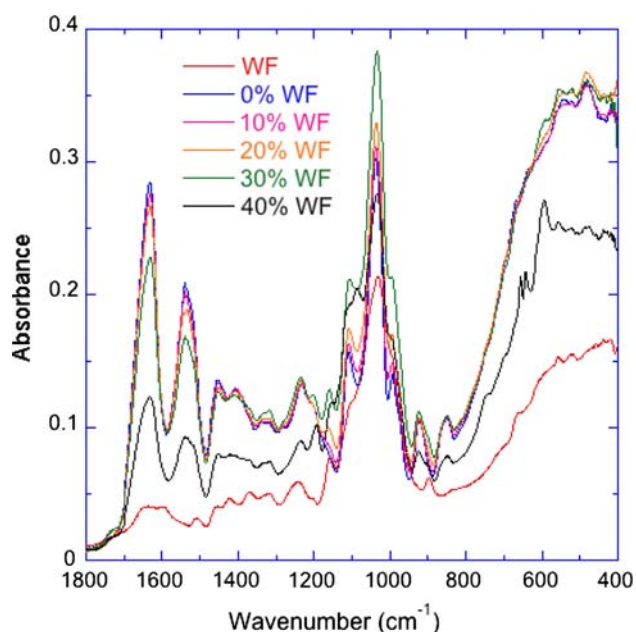


Fig. 9 Amide region of FKP composites with 53 μm wheat straw fibers at various fiber loadings

although there could be contributions from other hydroxyls given that there were multiple sources. Three $\nu(\text{C}-\text{O})$ peaks around 1,100, 1,050, and 1,000 were present in all samples. The 1,100 cm^{-1} peak originated exclusively in glycerol because it was not a prominent peak in lignocellulose. As fiber loading increased, the 1,050 cm^{-1} peak did not shift, the 1,000 cm^{-1} peak transitioned from a definitive peak to a shoulder on the larger 1,050 cm^{-1} peak, and the 1,100 cm^{-1} peak shifted down in wavenumber to 1,087 cm^{-1} . The appearance of the 1,200 and 600 cm^{-1} peaks and the shift of the 1,100 cm^{-1} peak suggested that interactions between polymer and fiber phases were happening between phenols on lignin and hydroxyls in FKP. The most likely interaction was through glycerol. Some glycerol leaching into the fibers would make surface phenols from lignin easier to vibrate thus new peaks appeared. The shift of the hydroxyl peak at 1,100 cm^{-1} meant that one of the hydroxyls on glycerol in FKP now existed in a new state. The more accessible C–O and O–H on phenols and O–H on glycerol provided a new hydrogen-bonding interaction between the phases evidenced by FT-IR. This new interaction was the major contributor to the reinforcement in modulus observed at high fiber loadings or moderate loadings of long fibers.

Conclusions

This study revealed that reinforcement of protein-based plasticized polymer matrices can occur using long

lignocellulosic fibers and/or high fiber loadings. FT-IR showed that these conditions had some moderate hydrogen-bonding interactions between the fiber and polymer. However, reinforcement could only occur at small strain loadings and a shear lag analysis showed that most of the interaction between the fiber and polymer was through friction. To get realistic comparisons of the fiber reinforcing efficiency on the plasticized protein matrix, composite properties must be normalized by un-reinforced matrix properties at the same plasticizer level.

Acknowledgements The authors wish to thank Maria Medynets of the USDA-ARS for the preparation and tensile testing of the composites, Eric Erbe of the USDA-ARS for the SEM experiments, and Elijah Morrison of Virginia Tech for the FT-IR and TGA experiments of the composites. The generous support of the Poultry Protein and Fat Council of the U.S. Poultry and Egg Association and VT-ICTAS is greatly appreciated.

References

1. The Economist (2007) The end of cheap food, Dec. 6, 2007
2. Market Trends (2007) Biofuels Bioprod Bioref 1:8
3. Parkinson G (1998) Chem Eng 105:21
4. Barone JR, Schmidt WF, Liebner CFE (2005) J Appl Polym Sci 97:1644–1651
5. Barone JR, Schmidt WF, Gregoire NT (2006) J Appl Polym Sci 100:1432–1442
6. Bledzki AK, Gassan J (1999) Prog Polym Sci 24:221–274
7. Mohanty AK, Misra M, Drzal LT (2002) J Polym Environ 10:19–26
8. Barone JR, Schmidt WF (2005) Comp Sci Tech 65:173–181
9. Shanks RA, Hodzic A, Wong S (2004) J Appl Polym Sci 91:2114–2121
10. Lu Y, Weng L, Cao X (2006) Carb Polym 63:198–204
11. Jansson A, Thuvander F (2004) Carb Polym 56:499–503
12. Wool RP, Sun XS (2005) Bio-Based Polymers and Composites. Elsevier, Amsterdam, pp 396–403
13. Bigi A, Borghi M, Cojazzi G, Fichera AM, Panzavolta S, Roveri N (2000) J Therm Anal Cal 61:451–459
14. Taylor MM, Liu CK, Marmer WN, Brown EM (2003) J Am Leather Chem Soc 98:435–444
15. Tanabe T, Okitsu N, Yamauchi K (2004) Mater Sci Eng C 24:441–446
16. Chabba S, Netravali A (2005) J Mater Sci 40:6253–6273
17. Angles MN, Dufresne A (2000) Macromolecules 33:8344–8353
18. Angles MN, Dufresne A (2001) Macromolecules 34:2921–2931
19. Averous L, Boquillon N (2004) Carb Polym 56:111–122
20. Huang M, Yu J (2006) J Appl Polym Sci 99:170–176
21. Lodha P, Netravali A (2002) J Mater Sci 37:3657–3665
22. Noishiki Y, Nishiyama Y, Wada M, Kuga S, Magoshi J (2002) J Appl Polym Sci 86:3425–3429
23. Lu X, Zhang MQ, Rong MZ, Shi G, Young GC (2002) J Polym Comp 23:624–633
24. Cinelli P, Chiellini E, Lawton JW, Imam SH (2006) Polym Deg Stab 91:1147–1155
25. Barone JR, Schmidt WF (2005) Comp Sci Tech 65:171–181
26. Barone JR, Schmidt WF, Liebner CFE (2005) Comp Sci Tech 65:683–692
27. Chawla KK (1987) Composite materials. Springer-Verlag, New York, pp 200–202, 233–235

28. Cox HL (1952) *Brit J Appl Phys* 3:72–79
29. Nardone VC, Prewo KM (1986) *Scripta Metal* 20:43–48
30. Sain M, Panthapulakkal S (2006) *Ind Crop Prod* 23:1–8
31. Fischer H, Polikarpov I, Craievich AF (2004) *Protein Sci* 13:2825–2828
32. Doi M, Edwards SF (1986) *The theory of polymer dynamics*. Clarendon Press, Oxford, pp 324–326
33. Gunzler H, Gremlich H-U (2002) *IR spectroscopy*. Wiley-VCH, Weinheim, pp 203–240